Interfacial Properties and Microfailure Degradation Mechanisms of Bioabsorbable Composites for Implant Materials using Micromechanical Technique and Acoustic Emission

Dae-Sik Kim[*], Joung-Man Park[*,†], Sung-Ryong Kim[**]

Micromechanical 시험법과 Acoustic Emission 을 이용한 Implant 용 생흡수성 복합재료의 계면물성과 미세파괴 분해메카니즘

김대식[*] · 박종만[*,†] · 김성룡[**]

KEY WORDS: bioabsorbable composites, micromechanical techniques, acoustic emission (AE), interfacial shear strength (IFSS), hydrolysis, wettability

ABSTRACT

The changes of interfacial properties and microfailure degradation mechanisms of bioabsorbable composites with hydrolysis were investigated using micromechanical test and acoustic emission (AE). As hydrolysis time increased, the tensile strength, the modulus and the elongation of PEA and bioactive glass fibers decreased, whereas those of chitosan fiber changed little. Interfacial shear strength (IFSS) of bioactive glass fiber/poly-L-lactide (PLLA) composite was significantly higher than that two other systems. The decreasing rate of IFSS was the fastest in bioactive glass fiber/PLLA composite, whereas that of chitosan fiber/PLLA composite was the slowest. With increasing hydrolysis time, distribution of AE amplitude was narrow, and AE energy decreased gradually.

Nomenclature

τ	: Interfacial shear strength (IFSS)
α, β	: Scale and shape parameters in Weibull distribution
COV	: Coefficient of Variation
γ_c	: Critical surface tension
γ_s	: Surface free energy of Solid
γ_s^p, γ_s^d	: Polar and dispersive surface free energy
W_a	: Work of adhesion

1. INTRODUCTION

Bioabsorbable bone fixation, screw and rods can offer the major advantages over conventional metallic implants as follows: the need for removal surgery is obviated [1] and the financial savings [2]. In addition, the degradation products are biocompatible in contrast to harmful metallic ions [3] and the elastic modulus is closer to that of bone, which could minimize the stress concentration near the edge of the implants. Because the currently available absorbable polymer materials in alone have the insufficient modulus and the strength for certain demanding applications, bioabsorbable fiber reinforced composite materials has been investigated. It is very important to know the interfacial properties [4,5] and microfailure degradation mechanisms between bioabsorbable fiber and matrix as a function of hydrolysis time. Chu *et al.* [6] measured the decreasing IFSS of CaP or chitin fibers reinforced PLLA composite with hydrolysis by microdroplet and single-fiber composite (SFC) tests. Daniels [7] reported that the initial mechanical properties and degradation kinetics measured for the design of absorbable fracture fixation devices. AE is well known as one of the important

[*] Department of Polymer Science and Engineering, Research Center for Aircraft Parts Technology, Gyeongsang National University

[**] Polymeric Materials Group, Central Research & Development, Samyang Corporation

[†] To whom correspondence should be addressed

nondestructive testing methods [8]. AE can monitor the fracture behavior of a composite structure, and characterize AE parameters to understand the type of fracture sources and their progressing. In this work, interfacial properties and microfailure degradation mechanisms of the bioabsorbable composites for implant materials were investigated using micromechanical technique and nondestructive evaluation.

2. EXPERIMENTAL

2. 1. Materials

PEA fiber (3M Co.), commercially available for surgical suture and chitosan fiber (RC-Biochemical Co., Korea) were used, and their average diameters were 32.3 and 15.2 μm, respectively. Bioactive glass fiber (Institute of biomaterials, Finland) as ceramic-type bioabsorbable fiber was used to compare to bioabsorbable polymeric fiber and Average diameter was 40.0 μm. PLLA (Sigma-Aldrich Co.) was used as matrix and their average molecular weight was from 85,000 to 160,000. The melting temperature (T_m) of PLLA is about 180°C and the glass transition temperature (T_g) is about 57°C.

2. 2. Methodologies

2. 1. 1. Measurement of Single-Fiber Tensile Strength under Hydrolysis: PEA, chitosan and bioactive glass fibers were fixed on the acryl frame using Kapton tape, and they were hydrolyzed in deionized water. In order to accelerate the degradation, the vacuum oven was used at elevated temperature, 70°C. The degradation time was ranged as the initial state, 1, 3, 5 and 10 days, respectively. The tensile strength of bioabsorbable fibers with hydrolysis time and various gauge lengths was obtained using about fifty specimens for statistically meaningful value.

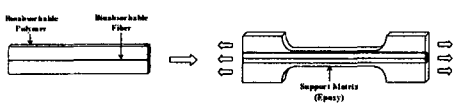

Fig. 1 Schematic figure of DMC specimen.

2. 2. 2. Measurement of IFSS: Double-matrix composites (DMC) test was applied to measure the IFSS between bioabsorbable fiber and matrix. Figure 1 shows schematic figure of DMC specimen. Bioabsorbable fiber was coated using PLLA solved in dimethylchloride. Hydrolysis temperature was established in the incubator at 37°C. The degradation time was ranged as the initial state, 5, 10, 15 and 20 days at evaluating temperature, respectively. Bioabsorbable fiber coated PLLA was embedded in epoxy resin and then cured for 3 days at room temperature. Epoxy resin was used as only supporting matrix to apply DMC test.

The IFSS of bioabsorbable fibers/PLLA composites was calculated from Drzal Eq. (1) [9]. Results obtained from DMC test assume to be similar to those of SFC test and it has advantages such as saving expensive bioabsorbable matrix as well as testing time.

$$\tau = \frac{\sigma_f}{2 \cdot \alpha} \cdot \Gamma \left[1 - \frac{1}{\beta} \right] \tag{1}$$

2. 2. 3. Measurement of Wettability: Wettability of bioabsorbable fiber and matrix was measured by Wilhelmy plate method (Sigma 70, KSV Co.). Dynamic contact angle, critical surface tension and polar and dispersive surface free energy of the fiber were measured. Since buoyancy force value is zero at the immersing interface, Wilhelmy equation can be modified as follows:

$$\cos\theta = \frac{M \cdot g}{\pi D \gamma_{LV}} \tag{2}$$

where M is measured force. The value of critical surface tension at $\cos\theta = 1$ was measured using Zisman plot that plotted γ_{LV} *versus* $\cos\theta$. To measure polar and dispersive surface free energies, Owens-Wendt Eq. (3) were expressed as follows:

$$W_a = 2\sqrt{\gamma_l^d \gamma_s^d} + 2\sqrt{\gamma_l^p \gamma_s^p} \tag{3}$$

where W_a is work of adhesion, γ_l, γ_l^d and γ_l^p is known for the testing liquids and $\cos\theta$ can be measured using Eq. (2). Polar and dispersive surface free energy can be measured from the slope and the intercept of the graph, where $(\sqrt{\gamma_l^p}/\sqrt{\gamma_l^d})$ and $(W_a/2\sqrt{\gamma_l^d})$ are plotted by Eq. (3).

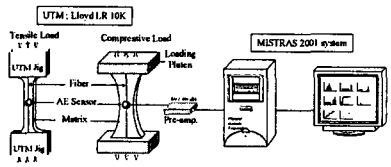

Fig. 2 Experimental system for AE test

2. 2. 4. AE Measurement: Figure 2 shows experimental set up of AE test in tensile and compressive tests. Specimen was placed on the universal testing machine (UTM) for tensile and compressive tests. AE sensor was attached at the center of the specimen using a vacuum grease couplant. AE signals were detected by a miniature sensor (Resonance Type, R15 model by PAC) with peak sensitivity of 69 Ref. V/(m/s) and resonant frequency at 150 kHz. The sensor output was amplified by 60 dB at preamplifier and passed through a band-pass filter with a range of 50 kHz to 200 kHz. The threshold level was set as 30 dB. Then the signal was fed into an AE signal

process unit (MISTRAS 2001 System) and AE parameters were analyzed using in-built software.

3. RESULTS AND DISCUSSION

3. 1. Mechanical Properties of Bioabsorbable Fibers with Hydrolysis: The mechanical properties of PEA, chitosan and bioactive glass fibers as a function of hydrolysis time at 70°C are shown in figures 3. The tensile strength, the modulus and the elongation of PEA fiber decreased continuously. It might be due to the increasing brittleness resulted from decreasing molecular weight as hydrolysis continued. The mechanical properties of chitosan fiber changed little with testing time. In the bioactive glass fiber, the mechanical properties decreased very steeply because degradation rate was the fastest.

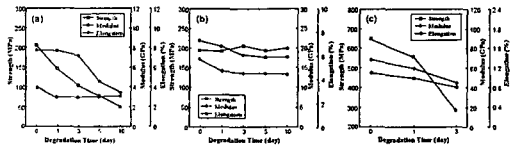

Fig. 3 The mechanical properties of bioabsorbable (a) chitosan, (b) PEA, and (c) bioactive glass fibers

In figure 4 (a), bimodal Weibull distribution exhibited for three degradation conditions. The bimodality appeared in the whole degradation ranges. After 10 days, distribution curve is similar to unimodal distribution due to the increasing low-strength portion coming from increasing surface flaws, which acts as stress concentration. Figure 4 (b) shows scanning electron microscopy (SEM) photograph of PEA fiber after sufficient hydrolysis continued. Microcracks were propagated into the fiber along cross-sectional plane. Hydrolytic resistance is rather weak in cross-sectional direction of fiber because amorphous regions are less dense than the crystalline domains.

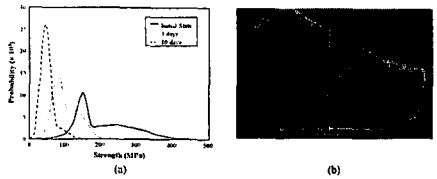

Fig. 4 (a) Bimodal Weibull distribution and (b) SEM photograph of PEA fiber

3. 2. IFSS and Microfailure Modes: Figure 5 (a) shows the change of IFSS for PEA, chitosn or bioactive glass fibers/PLLA composite with hydrolysis time in DMC test. IFSS between bioactive glass fiber and PLLA was significantly higher than that two other systems. It might be due to higher hydrogen bonding. IFSS of chitosan fiber/PLLA composite might be higher than that of PEA/PLLA composite. It might be because chitosan fiber has higher surface roughness that induced mechanical interlocking compared to relatively smooth surface of PEA fiber. As hydrolysis time increased, the decreasing rate of IFSS was the fastest for bioactive glass fiber/PLLA composite, whereas that of chitosan fiber/PLLA composite was the slowest. It means that interfacial degradation was the fastest comparing to two other systems. Hydrolytic resistance at the interface could be weak because bioactive glass fiber contains high hydrophilic groups such as SiO_2.

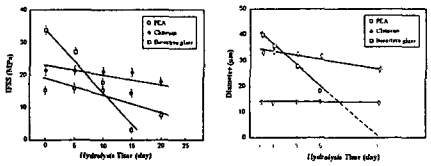

Fig. 5 Changes of (a) IFSS and (b) diameter

Figure 5 (b) shows decrease of diameter for PEA, chitosan and bioactive glass fibers with hydrolysis time at 70°C. PEA fiber decreased slightly and chitosan fiber changed little, whereas that of bioactive glass fiber decreased rapidly.

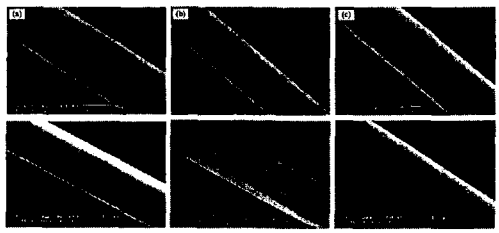

Fig. 6 SEM photographs of (a) PEA, (b) chitosan and (c) bioactive glass fibers before and after hydrolysis

Figure 6 shows SEM photographs of PEA, chitosan and bioactive glass fibers before and after hydrolysis at 70°C. It shows rougher surface of chitosan fiber compared to PEA and bioactive glass fibers. After 5 days, bioactive glass fiber exhibited rough surface, whereas surface roughness of PEA and chitosan fibers changed little until 10 days.

Figure 7 shows the typical microfailure modes of PEA fiber (a) at the initial state, (b) after 5 days and (c) after 10 days. At the initial state, PEA fiber showed ductile microfailure mode such as diagonal fracture, whereas at 10 days vertical fracture appeared because of the increasing brittleness based on hydrolysis. The number of fragments increased with increasing hydrolysis time.

Figure 8 shows typical microfailure modes of

bioactive glass fiber in (a) tensile and (b) compressive tests. In tensile test, brittle microfailure modes such as vertical fracture appeared, whereas fiber slippage was observed in compressive test.

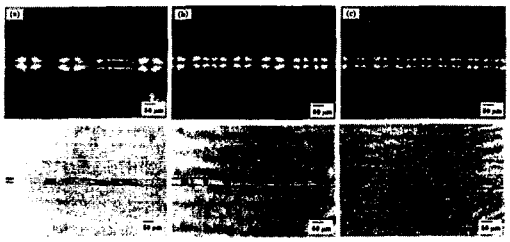

Fig. 7 The typical microfailure modes for PEA fiber

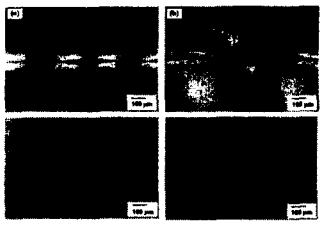

Fig. 8 The typical microfailure modes for bioactive glass fiber in (a) tensile and (b) compressive tests

3. 3. Surface Wettability and Adhesion: It is considered that the better wettability, the higher interfacial adhesion. Tables 1 and 2 show surface free energies, critical surface tension and work of adhesion for bioabsorbable fibers and matrix. Critical surface tension and polar surface free energy of bioactive glass fiber was higher than the other two fibers. Work of adhesion, W_a between bioactive glass fiber and PLLA was also the highest. These trends are consistent with IFSS results.

Table 1 Surface free energies and critical surface tension of bioabsorbable fibers and matrices

Biomaterials		γ_c (dyn/cm)	γ_s^d (mJ/m^2)	γ_s^p (mJ/m^2)	γ_s (mJ/m^2)
Fiber	PEA	32.9	22.3	15.9	38.2
	Chitosan	53.5	43.3	9.0	52.3
	Bioactive glass	55.3	35.6	19.1	54.7
Matrix	PLLA	35.8	26.2	7.7	33.9

Table 2 Work of adhesion, W_a for the bioabsorbable fibers and matrix

W_a (mJ/m^2)	Matrix	Fiber		
		PEA	Chitosan	Bioactive glass
	PLLA	70.5	84.0	85.3

3. 4. AE Outcomes: It was interested in measuring the sequence of bioabsorbable fiber fracture to correlate the AE events with the different failure modes. Figures 9 and 10 show AE amplitude and energy of PEA and chitosan fibers with measuring time (a) at the initial state and (b) after 10 days. For PEA fiber, distribution of AE amplitude became narrow and AE energy decreased with increasing hydrolysis time. Distribution of AE amplitude might be broad due to diagonal fracture, whereas vertical fracture might make AE amplitude distribution to be narrow. For chitosan fiber, AE amplitude and energy changed little. It is because mechanical properties of chitosan fiber did not change significantly with hydrolysis time.

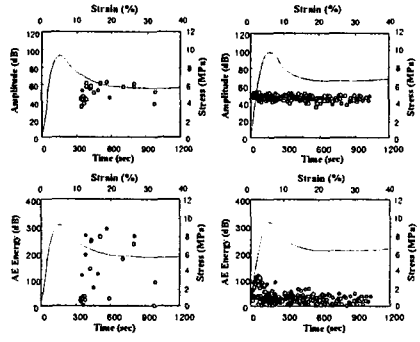

Fig. 9 AE amplitude and energy for PEA fiber

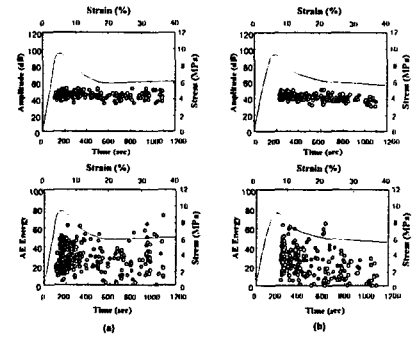

Fig. 10 AE amplitude and energy for chitosan fiber

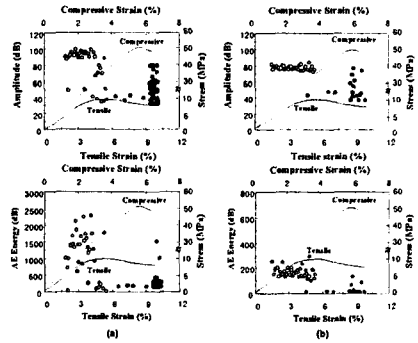

Fig. 11 AE amplitude and energy for bioactive glass fiber

Figure 11 shows AE results for bioactive glass fiber with stress-strain curves using the tensile/compressive tests (a) at the initial state and (b) after 3 days. For both the initial and after degradation cases, AE amplitude and

energy in tensile failure may be much higher than those of compressive test. It is probably because of the difference in fracture modes and energies between the longitudinal tensile loading in tensile test and the transverse tensile loading in compressive test. Fiber breaks occurred until just before yielding point in tensile test. Beyond yielding point, AE events were not detected because of the absence of interlayer and matrix failures under tensile test, whereas incase of compressive test, AE events occurred from interlayer failure and matrix buckling. AE amplitude and energy at the initial state may be much higher than that of after degradation for two type test methods. It might be due to the difference in fracture energy by the hydrolysis.

4. CONCLUSIONS

As hydrolysis time increased, the mechanical properties of bioactive glass fibers decreased steeply and those of PEA fiber decrease gradually, whereas those of the chitosan fiber changed little. IFSS between bioactive glass fiber and PLLA was significantly higher than two other systems. The decreasing rate of IFSS was the fastest in bioactive glass fiber/PLLA composite and that of chitosan fiber/PLLA composite was the slowest. Although interfacial properties of bioactive glass fiber with hydrolysis were rather poor, mechanical properties such as modulus and strength were strong. In the case of the hydrolytic resistance is improved, bioactive glass fiber/PLLA composite could be applicable to bioabsorbable composites for implant materials. PEA fiber appeared ductile microfailure modes at the initial state, whereas brittle microfailure modes appeared with increasing hydrolysis time. Distribution of AE amplitude was narrow and AE energy decreased gradually. It may be due to the decreasing fiber fracture energy as well as the change of microfailure modes.

ACKNOWLEDGMENT: This work was financially supported by Research Center for Aircraft Parts Technology (ReCAPT).

REFERENCES

1. O. Bostman, E. A. Makela, P. Tormala and P. Rokkanen, Brief report. *J. Bone Joint Surg.*, Vol. 71B, 1989, p. 706.
2. O. M. Bostman, *Scand, J. Soc. Med.*, Vol. 22, 1992, p. 41.
3. K. Sinibaldik, H. Rosen, S. K. Lin and M. De Angelis, *Clin. Orthop. Rel. Res.*, Vol. 118, 1976, p. 257.
4. J. M. Park, W. G. Shin, and D. J. Yoon, *Compos. Sci. & Technol.*, Vol. 59, 1999, p. 355.
5. J. M. Park and D. S. Kim, *Polym. Compos.*, Vol. 21, No. 5, 2000, p. 789.
6. M. A. Slivka, C. C. Chu and I. A. Adisaputro, *J. Biomedical Mater Res.*, Vol. 36, 1997, p. 469.
7. K. P. Andriano, K. H. Wenger, A. U. Daniels and J. Heller, *J. Biomedical Mater Res.*, Vol. 48, 1999, p. 528.
8. B. T. Ma, L. S. Schadler, C. Laird and J. C. Figueroa, *Polym. Compos.*, Vol. 11, 1990, p. 211.
9. L. T. Drzal, M. J. Rich, M. F. Koenig and P. F. Lloyd, *J. Adhesion*, Vol. 16, 1983, p. 133.